Nitrogen Oxide Abatement by Distributed Fuel Addition

Contract DE-AC22-87PC79850

Quarterly Report No. 12

for Period

May 1, 1990 through July 31, 1990

Prepared by

J. O. L. Wendt and J. B. Mereb
Department of Chemical Engineering
University of Arizona
Tucson, Arizona 85721

Submitted to

Diane Revay Madden, Project Officer
Environmental Control Technology Division
Pittsburgh Energy Technology Center
Department of Energy

August 27, 1990

MASTER

SUMMARY

This quarterly report presents an overview of all our most important findings so far, in the format of a paper which is to be presented at the VGB Congress, Power Plants, 1990, to be held in Essen, West Germany from 18 through 21 September, 1990. A copy of the paper to be presented follows, and this will be published in the proceedings.

REBURNING MECHANISMS IN A PULVERIZED COAL COMBUSTOR

NACHVERBRENNUNGSMECHANISMEN BEI DER KOHLENSTAUBVERBRENNUNG

Jost O.L. Wendt and Jamal B. Mereb,
Department of Chemical Engineering,
University of Arizona,
Tucson, AZ 85718, USA.

Presented at

VGB-Kongreß Kraftwerke 1990,
Essen, BRD.

18 - 21 September 1990

REBURNING MECHANISMS IN A PULVERIZED COAL COMBUSTOR

Jost O.L. Wendt[1] and Jamal B. Mereb[2]
Department of Chemical Engineering
University of Arizona
Tucson, AZ 85721, USA.

ABSTRACT

The research reported here is concerned with the application of secondary fuel addition, otherwise known as reburning, as a means of NO_x destruction downstream of the primary flame zone in boilers. This paper consists of two parts: First, results from a statistically correct design of parametric experiments on a laboratory coal combustor are presented. These allow the effects of the most important variables to be isolated and identified. Second, mechanisms governing the inter-conversion and destruction of nitrogenous species in the fuel rich reburning zone of a laboratory coal combustor were explored, using fundamental kinetic arguments. The objective here was to extract models, which can be used to estimate reburning effectiveness in other, more practical combustion configurations.

Emphasis is on the use of natural gas as the reburning fuel for a pulverized coal primary flame. Then, reburning mechanisms occur in two regimes; one in which fast reactions between NO and hydrocarbons are usually limited by mixing; the other in which reactions have slowed and in which known gas phase chemistry controls. For the latter regime, a simplified model based on detailed gas phase chemical kinetic mechanisms and known rate coefficients was able to predict temporal profiles of NO, NH_3 and HCN. Reactions with hydrocarbons played important roles in both regimes and the Fenimore N_2 fixation reactions limited reburning effectiveness at low primary NO values.

INTRODUCTION

Reburning[1] is an NOx abatement technique in which secondary fuel is injected downstream of the fuel lean primary combustion zone of a pulverized coal boiler. This form of NOx abatement has been applied to full-scale units[2,3] and appears to be especially attractive when natural gas is used as the reburning fuel to destroy pollutants created from pulverized coal combustion.

---

[1] Professor of Chemical Engineering, to whom correspondence concerning this paper should be addressed.

[2] Graduate Student

The effectiveness of this process is determined by a large number of combustion variables. Therefore, a preliminary investigation is required to yield a superficial understanding of which variables are important, and to what extent. Empirical modeling derived from a statistical design of experiments can be a useful procedure to accomplish this, provided that care is taken not to extrapolate results beyond the parameter domain in which they were measured.

A more general insight to the process is achieved through a more fundamentally based modelling approach. Therefore, the research reported here is also concerned with a quantitative delineation of mechanisms that control the destruction and formation of all nitrogenous species in the reburning zone downstream of a pulverized coal flame in a laboratory combustor. The focus is on natural gas reburning[4,5], with the objective of creating engineering models that are both fundamentally based and yet are sufficiently simple so that they can be used in more complex models of practical combustors.

Among other issues, we address the following: What is the relative contribution of hydrocarbons versus other combustible species in governing NO destruction? What controls the formation and destruction of HCN at both high and low primary NO values? What are the key salient mechanisms describing the formation and destruction of NH_3, HCN and NO in the reburning zone for a pulverized coal primary flame?

Mechanisms governing the destruction of NO in the far fuel rich post flame of a pulverized coal staged combustion system were delineated by Bose and Wendt[6]. They based their analysis on the pioneering fundamental gas phase kinetics studies of others (Glarborg et al.[7], Fenimore[8], Haynes[9,10], among others). The current work extends their analysis to a reburning configuration, and expands the analysis to predict both HCN and NH_3 concentrations as well.

EXPERIMENTAL COMBUSTOR

Space limitations preclude other than a very brief discussion of the 15 cm ID laboratory combustor, which is similar to that described elsewhere[6]. In essence, the combustor allowed self-sustaining combustion of 1-2 kg/h coal with no external heating, in a plane flame configuration that was representative of full-scale units in terms of temperature time history. A schematic is shown on Figure 1.

The first stage (pulverized coal), was operated fuel lean and reburning (secondary) fuel (natural gas, CO or H_2) was injected downstream. Variable amounts of N_2 were added to the reburn fuel and this resulted in adequate mixing within 0.18 s, beyond which radial profiles demonstrated that the furnace did exhibit plug flow reactor behavior, at least as far as temperature and concentration profiles were concerned.

5

Analyses of major (O_2, CO, CO_2 and H_2) and minor (CH_4, C_2H_6, C_2H_2, NO, HCN, NH_3, and N_2O) species were obtained using a water cooled, water quenched probe, continuous emission monitors, two gas chromatographs furnished with TC, FID, and ECD detectors, and ion and gas specific electrodes. Temperature measurements were made using an uncoated Type R thermocouple, corrected for radiation losses. Time resolution of temperature and species profiles was determined by the distance between access ports in the combustor (0.3 - 0.4 s). Utah Bituminous coal was used for the primary flame.

PRELIMINARY INVESTIGATION USING STATISTITICAL EXPERIMENTATION

In order to explore mechanisms which govern the destruction of NO, it is useful first to determine the individual contributions to NO abatement of each of the variables that are associated with reburning. For this purpose, a statistically designed parametric investigation was conducted. A Central Composite Experimental Design was used to study the effect of process variables on the overall reduction in NO by reburning. The results were used to define optimum conditions and to identify the significant variables affecting NO reduction by reburning.

Empirical correlations, fitted to data, yielded response curves which allowed the examination of the effect of each process variable separately. The response was defined as:

$$Y = 100 - 100 * (NO_{exhaust}/NO_{primary})$$

where all NO concentrations have been corrected for dilution. Exhaust values were after final air addition and primary values denote those leaving the primary coal flame zone. Significant variables were stoichiometries in the primary zone and in the reburn zone and reburn zone temperature and residence time. Other variables did not show statistical significance in the experimental range that was covered and were not included in the analysis.

Contour plots on Figure 2 show the NO reduction response as a function of reburn zone temperature and residence time. The data points are included to show the experimental range that was covered and are not representative of how the predictions compare to experiment. The plots indicate that residence time effects dominate at short residence times and temperature effects dominate at long residence times.

Figure 3 shows the importance of temperature and stoichiometric ratio in the reburning zone. Under the more fuel rich reburning zone conditions, higher temperatures lead to more NO destruction. Under the less fuel rich conditions, the effect of temperature is reversed. Figure 4 shows a comparison between the actual measured and the predicted response as a function of reburn zone stoichiometric ratio. The experimental data suggest an optimum stoichiometry of about 0.8, and this was not predicted by the correlation,

6

because it was smoothed out by the non-linear regression. This demonstrates why an empirically based type of modelling is not always adequate to understand the process.

In short, a parametric study based on a statistical experimental design was an efficient method to yield a qualitative, rather than a quantitative, understanding of the reburning process. In order to understand the mechanisms which govern the destruction of NO in reburning, a theoretical study was undertaken, and this is the focus of the remainder of this paper.

During this phase of the work, on-line N_2O measurements were also made. Only very low values (generally less than 5 ppm) were observed, although an increase to 9 ppm was observed at the point of final air addition, for both air staged and reburning conditions.

MECHANISMS: EXPERIMENTAL RESULTS

In order to explore mechanisms, measurements of temperature and species concentrations were made at various axial positions down the combustor. This yielded time resolved profiles. In all, 14 runs under various conditions, with various reburning fuels, were completed. Reburning fuel was injected 0.5 - 0.6 s downstream from the primary coal flame. In the reburn zone, temperatures ranged from 1380 to 1520 K at the entrance and from 1200 to 1280 K at the exit. Typical profiles are depicted by the data points in Figure 5 which show nitrogenous species profiles for three cases in which the primary flame was coal and the reburning fuel was natural gas. Time zero is the inlet to the reburning zone, where the primary NO (not depicted on the graphs in order to maintain appropriate scales) is noted in each figure as NO_p. Reburn zone stoichiometry, SR_r, is also noted in each figure. Clearly, there are two regimes which come under consideration. First, for the regime covered by the profiles on the graph, there are no mixing complications, and species change over fairly long time scales. Second, between the inlet to the reburning zone (NO_p) and the first data point there is a very rapid destruction of NO, and here mixing effects might be important, since time scales are short (within 0.18 s). Note the rise of HCN and NH_3 in the slow kinetic regime.

Figure 6 shows reburning zone profiles with CO and H_2 as the reburning fuels. The HCN and NH_3 values are extremely small (less than 7 ppm for HCN and less than 16 ppm for NH_3), which is to be expected since hydrocarbon values in the reburning zone were less than 100 ppm. Carry over of char nitrogen from the primary flame is therefore, at most, only a minor contributor to HCN formation in the reburn zone.

In order to explore other possible sources of HCN formation, some experiments replaced coal in the primary flame by natural gas, where the primary NO could be adjusted by doping with NH_3. In Figure 7, the primary NO is only 24 ppm, but the HCN produced in the reburning zone is in excess of 40 ppm, corresponding to fractional conversions much higher than 100%. Fractional conversion is the ratio of the molar rate of the nitrogenous

species to that of the primary NO and TFN (total fixed nitrogen) is the sum of NO, HCN and NH_3 concentrations. Thus, nitrogenous species inter-conversion reactions cannot account for all the formation of HCN. Clearly, Fenimore[11] fixation of N_2 produces HCN which can limit the destruction of nitrogenous species by reburning, and this agrees with the interpretation of package boiler data by Lanier et al.[5]. Figure 8 shows the effects of changes in NO_p and, together with other data, is used later to compare with the predictions of a model.

DATA ANALYSIS AND MODEL DEVELOPMENT
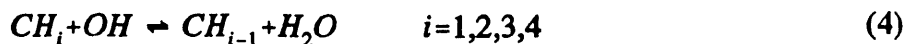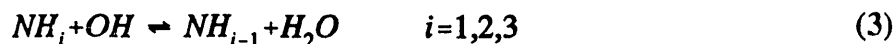
Slow Kinetic Regime (No Mixing Complications)

For this regime we take as our initial point the first data point after reburning fuel has been introduced, and attempt to predict the subsequent profiles of NO, HCN and NH_3. The objective is to determine which mechanisms control the conversion of nitrogenous species in long time scales.

Following Bose and Wendt[6], we use the detailed kinetic mechanism of Glarborg, Miller and Kee[7] as a basis for determining both, which reactions were likely to be most important, and values of kinetic rate coefficients to be employed. No adjustment of any rate constant is made and the analysis is done only in terms of known detailed kinetic mechanisms taken from the literature.

The rate of destruction of NO is given by:

$$NO+NH_i \rightarrow products \qquad i=0,1,2 \qquad\qquad (1)$$

$$NO+CH_i \rightarrow products \qquad i=0,1,2 \qquad\qquad (2)$$
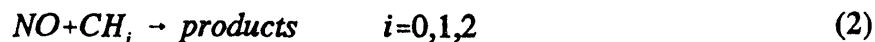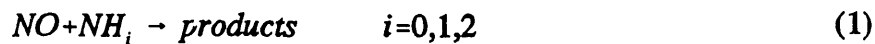
where NH_i and CH_i concentrations were calculated from partial equilibria:

$$NH_i+OH \rightleftharpoons NH_{i-1}+H_2O \qquad i=1,2,3 \qquad\qquad (3)$$

$$CH_i+OH \rightleftharpoons CH_{i-1}+H_2O \qquad i=1,2,3,4 \qquad\qquad (4)$$

This yields the following expression for the rate of change of NO:

$$\frac{d(NO)}{dt} = -(NO)(NH_3)f_1 - (NO)(CH_4)f_2 \tag{5}$$

which depends on the local NO, OH, CH_4, and NH_3 concentrations. Functions f_i, which depend on temperature, OH and H_2O concentrations, represent groupings of known elementary reaction rate constants and equilibrium constants and are shown on Table I.

HCN destruction rate was based on HCN + O reactions, HCN + OH reactions and the reversible reaction:

$$HCN + H \rightleftharpoons CN + H_2 \tag{6}$$
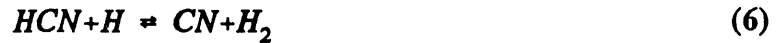
where CN was at a pseudo stationary state derived from Reaction (6), together with reactions CN + OH --> NCO + H and C + NO --> CN + O. Assumption of partial equilibrium was made for HCN + OH = CN + H_2O and O was assumed to be in partial equilibrium with H_2O and H_2.

HCN formation rate was based on Reaction (2) in addition to the reactions:

$$CH + N_2 \rightarrow HCN + N \tag{7}$$

$$CH_3 + N \rightarrow HCN + H + H \tag{8}$$

This yields the following expressions for the rates of change of HCN:

$$\frac{d(HCN)}{dt}\bigg|_{destruction} = -(HCN)[f_3 + f_4] \tag{9}$$

$$\frac{d(HCN)}{dt}\bigg|_{formation} = (CH_4)[(NO)f_2 + (N_2)f_5 + (NH_3)f_6] \tag{10}$$

N_2 was formed by Reaction (1) and destroyed by Reaction (7) yielding:

$$\frac{d(N_2)}{dt} = (NO)(NH_3)f_7 - (CH_4)(N_2)f_5 \tag{11}$$

The rate of change of NH_3 was determined from a nitrogen balance:

9

$$\frac{d(NH_3)}{dt} = -\frac{d(NO)}{dt} - \frac{d(HCN)}{dt} - 2\frac{d(N_2)}{dt} \tag{12}$$

The f_i in Equations (5 and 9-11) have the form:

$$f_i = \sum_{j=1}^{1,2,or3} A_{ij} T^{N_{ij}} \exp(\frac{B_{ij}}{T}) \times \frac{(OH)^{m_{ij}}}{(H_2O)^{l_{ij}}} \tag{13}$$

where values for parameters are shown on Table I. Equations (5 and 9-12) can predict XN species profiles, ab initio, provided initial conditions and estimates for OH are available. This is an extension of the previous analysis[6] which utilized measured NH_3 profiles, an empirical correlation for OH estimation and did not account for HCN formation due to Reactions (7 and 8).

Curve A on Figure 9 shows predictions based on OH being at equilibrium. Curve B uses a previous[6] empirical correlation for the OH equilibrium overshoot, while curves C and D calculate the OH concentration directly via OH + H + M --> H_2O + M, which was found to be the rate controlling OH recombination reaction[12]. H was in partial equilibrium with H_2O and H_2. This yields the following expression for OH decay:

$$\frac{d(OH)}{dt} = -(H_2)f_8 \tag{14}$$

where the initial OH concentration was calculated using measured NO decay rates from the gas flame data only, subsequent kinetic concentration of OH from Equation (14), and correlations of all these values. This yielded the following correlation for initial OH values:

$$\frac{(OH)_{initial}}{(OH)_{equilibrium}} = 12.185 \times 10^{-6} \times \exp(19109/T) \tag{15}$$

Simultaneous solution of the rates of change of OH, NO, HCN and NH_3 (Equations 5, 9-12 and 14) gives predictions of all nitrogenous species that are independent of their measured values (except at initial conditions). Curve C on Figure 9 excludes Reactions (7 and 8), and Curve D uses the expanded kinetic set described above. The NO decay is well predicted and the HCN profile does seem to require inclusion of Reactions (7) and (8).

Comparison of the lines shown on Figures 5,and 8 to the data, indicates that the above expressions are successful at predicting NO, HCN and NH_3 profiles in the reburning zone for a wide range of conditions, provided CH_4 is the reburning fuel. The symbols on Figure 10 show a comparison between theory and experiment for all 12 runs in which CH_4

was the reburning fuel, and indicate that the model did not bias the predictions to any particular species or experimental condition.

Fast Kinetic Regime (Possible Mixing Complications)

It is desired to predict the values of nitrogenous species at the first data point from the primary NO values. Using the above mechanism, predictions in which a lower bound of the initial OH was estimated by extrapolation, and in which the CH_4 concentration was taken either as the initial diluted value (assumes instantaneous perfect mixing) or the value at the first data point (assumes instantaneous oxidation of CH_4) yielded NO decay rates which were always far too rapid at the high NO_p values. Better predictions were obtained by assuming that CH_4 rose from 0 to the measured value below the injection point, which can only be true if mixing delays the contacting of NO_p with the reburning fuel. Although the kinetic model should not be used as a predictive tool as such, in this region, it demonstrates the limitations imposed by mixing, on NO reduction by hydrocarbon reactions.

CONCLUSIONS

Parametric studies showed that overall reburning effectiveness depended on reburning zone stoichiometry, temperature, and residence time, in a complicated manner in which the qualitative effects of one variable depended on the values of the other two.

During natural gas reburning in a practical coal combustor, NO destruction occurs in two regimes, one where mixing effects may be important and limit NO destruction, followed by one downstream where a simplified kinetic scheme, based on fundamental considerations, applies for NO, HCN and NH_3 concentrations. At low primary NO values, fixation of N_2 by hydrocarbons limits reburning effectiveness. Also, the $CH_3 + N$ reaction may make a significant contribution to HCN formation, depending on CH_4 and NH_3 concentrations. Hydrocarbons, however, are critical in destroying NO throughout the reburning zone, and this is consistent with the results of others[2,4,5] who used different experimental configurations and different primary fuels.

The proposed mechanism can be useful in predicting and optimizing reburning effectiveness, especially if mixing both at the reburning fuel injector and at the tertiary burn out air addition point can be simulated.

REFERENCES

(1)   Wendt, J.O.L., Sternling, C.V. and Matovich, M.A.: Fourteenth Symposium (International) on Combustion, p. 897, The Combustion Institute, 1973.

(2)   Miyamae, S., Ikebe, H., Makino, K., Suzuki, K. and Mogi, J.: Proceedings of the 1985 Joint Symposium on Stationary Combustion NOx Control, p. 24-1, EPRI, 1986.

(3)   Okigami, N., Sekiguchi, Y., Miura, Y., Sasaki, K. and Tamuru, R.: Proceedings of the 1985 Joint Symposium on Stationary Combustion NOx Control, p. 25-1, EPRI, 1986.

(4)   Chen, S.L., McCarthy, J.M., Clark, W.D., Heap, M.P., Seeker, W.R. and Pershing, D.W.: Twenty-First Symposium (International) on Combustion, p. 1159, The Combustion Institute, 1986.

(5)   Lanier, W.S., Mulholland, J.A. and Beard, J.T.: Twenty-First Symposium (International) on Combustion, p. 1171, The Combustion Institute, 1986.

(6)   Bose, A.C. and Wendt, J.O.L.: Twenty-Second Symposium (International) on Combustion, p. 1127, The Combustion Institute, 1988.

(7)   Glarborg, P., Miller, J.A. and Kee, R.J.: Comb. Flame, 65, 177, (1986).

(8)   Fenimore, C.P.: Seventeenth Symposium (International) on Combustion, p. 661, The Combustion Institute, 1979.

(9)   Haynes, B.S., Comb. Flame, 28, 81 (1977).

(10)   Haynes, B.S., Comb. Flame, 28, 113 (1977).

(11)   Fenimore, C.P.: Thirteenth Symposium (International) on Combustion, p. 373, The Combustion Institute, 1973.

(12)   Bose, A.C.: Pulverized Coal Combustion: Fuel Nitrogen Mechanisms in the Rich Post-Flame. Ph.D. Dissertation, University of Arizona, 1989.

TABLE I

Expressions for Functions f_i in the Form of

$$f_i = \sum_j f_{ij} \quad where \quad f_{ij} = A_{ij} T^{N_{ij}} \exp\left(\frac{B_{ij}}{T}\right) \times \frac{(OH)^{m_{ij}}}{(H_2O)^{l_{ij}}}$$

(units are g-moles, cm^3, seconds, Kelvins)

| i	j	A	N	B	m	l
1	1	3.3E17	-1.603	5277	1	1
	2	7.57E15	-0.917	19650	2	2
	3	3.20E12	-0.134	39105	3	3
2	1	5.83E14	-0.484	12436	2	2
	2	7.73E16	-0.678	20730	3	3
	3	1.20E14	-0.292	40708	4	4
3	1	9.20E12	0.0	-7549	1	0
	2	4.80E11	0.0	-5536	1	0
4	1	1.05E03	2.701	6283	2	1
	2	1.32E16	-0.695	-1327	2	1
5	1	1.34E14	-0.678	13886	3	3
6	1	1.25E15	-0.603	46200	4	4
7	1	1.18E17	-1.603	5277	1	1
	2	3.20E12	-0.134	39105	3	3
8	1	8.03E22	-2.511	7781	2	1

FIGURE CAPTIONS

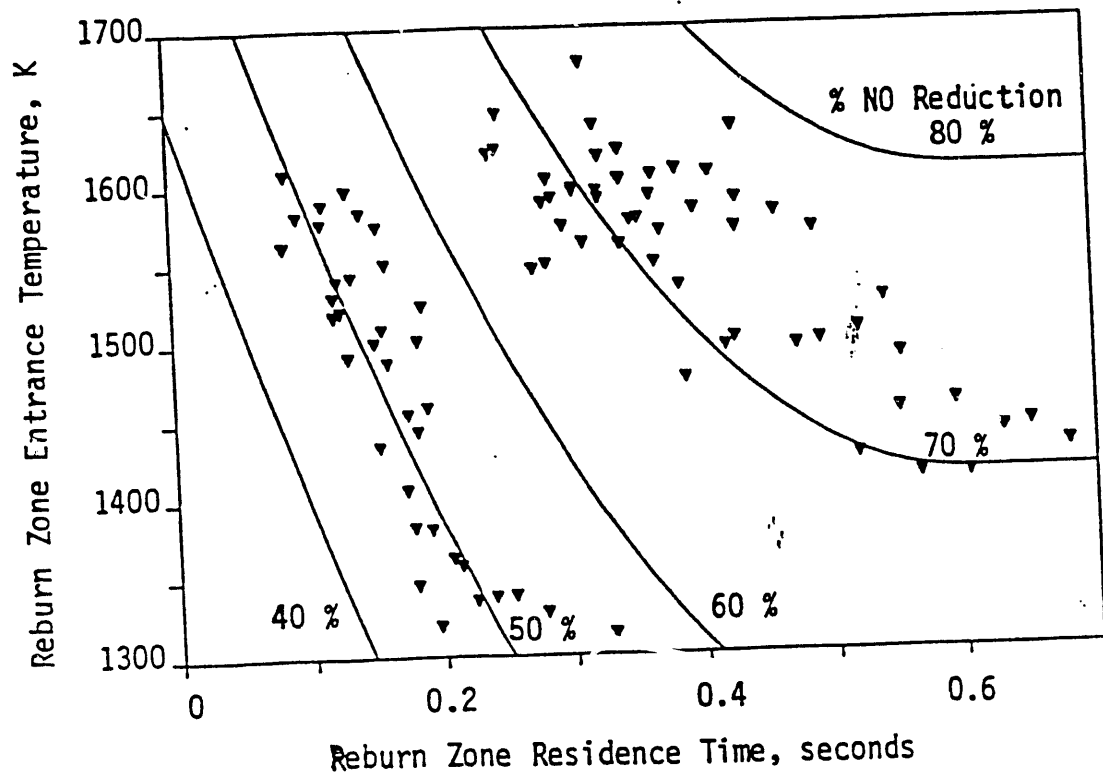FIG. 1.   Experimental Combustor.

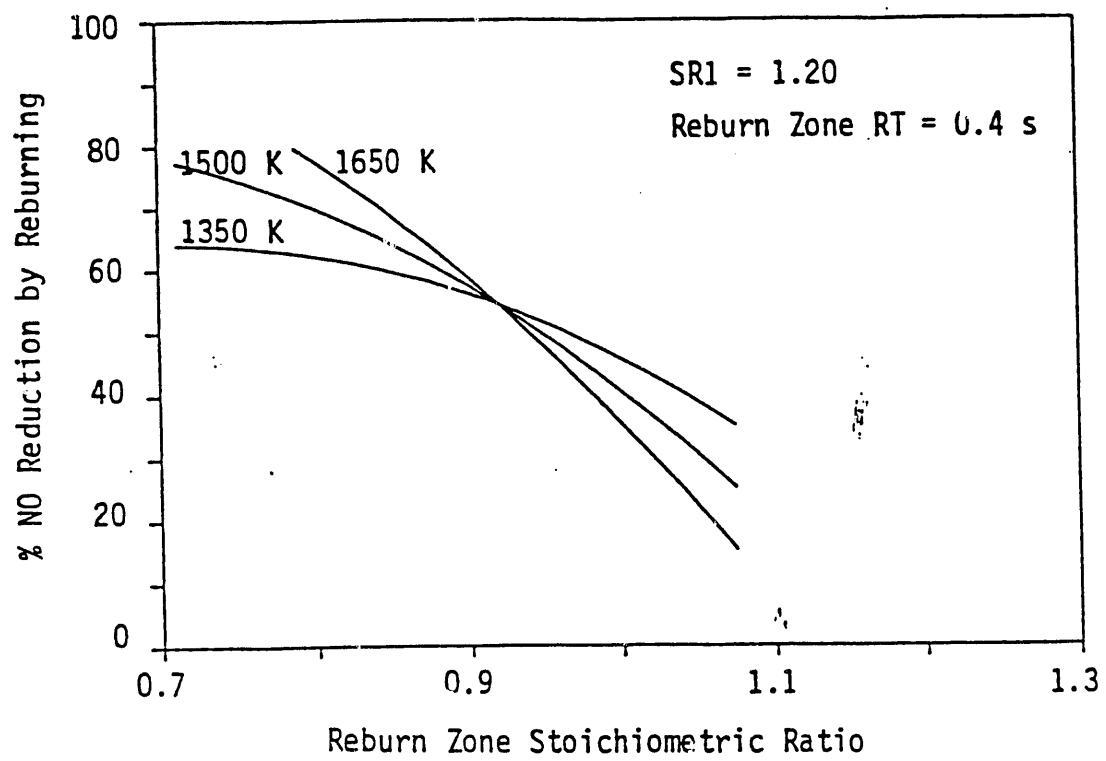FIG. 2.   Contour Plots for NO Reduction.

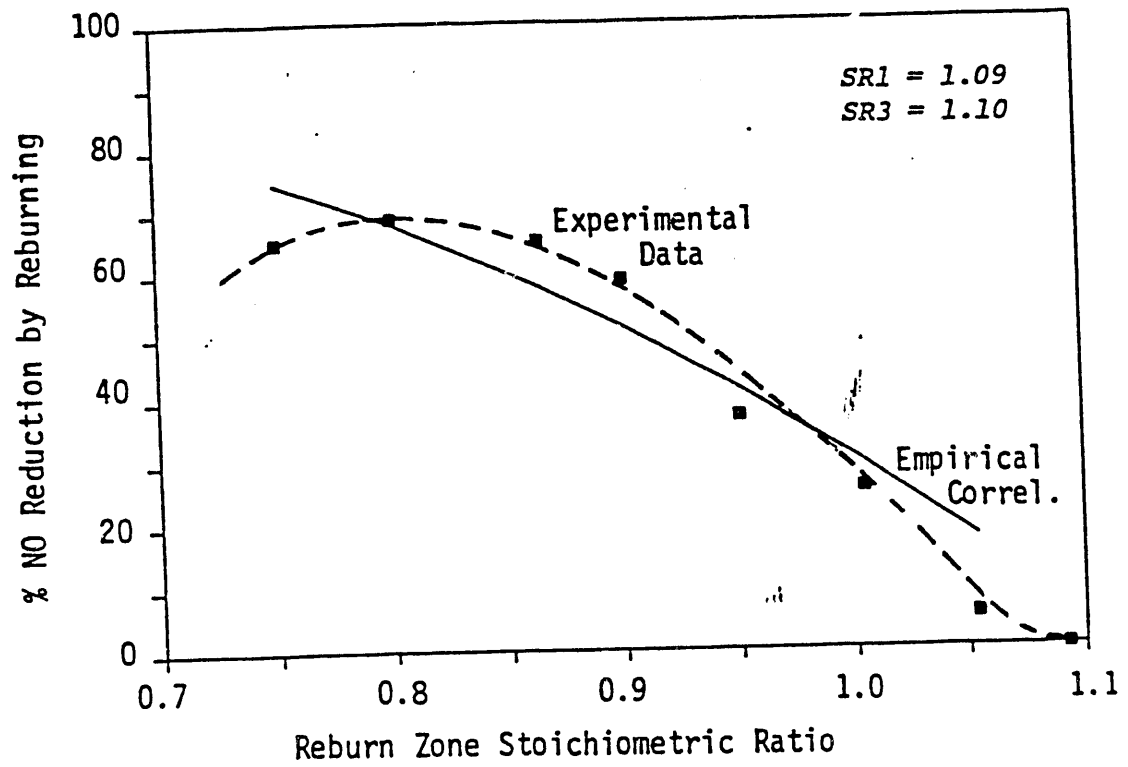FIG. 3.   Variation of NO Reduction with Reburn Zone Stoichiometric Ratio and Temperature.

FIG. 4.   Variation of NO Reduction with Reburn Zone Stoichiometric Ratio.
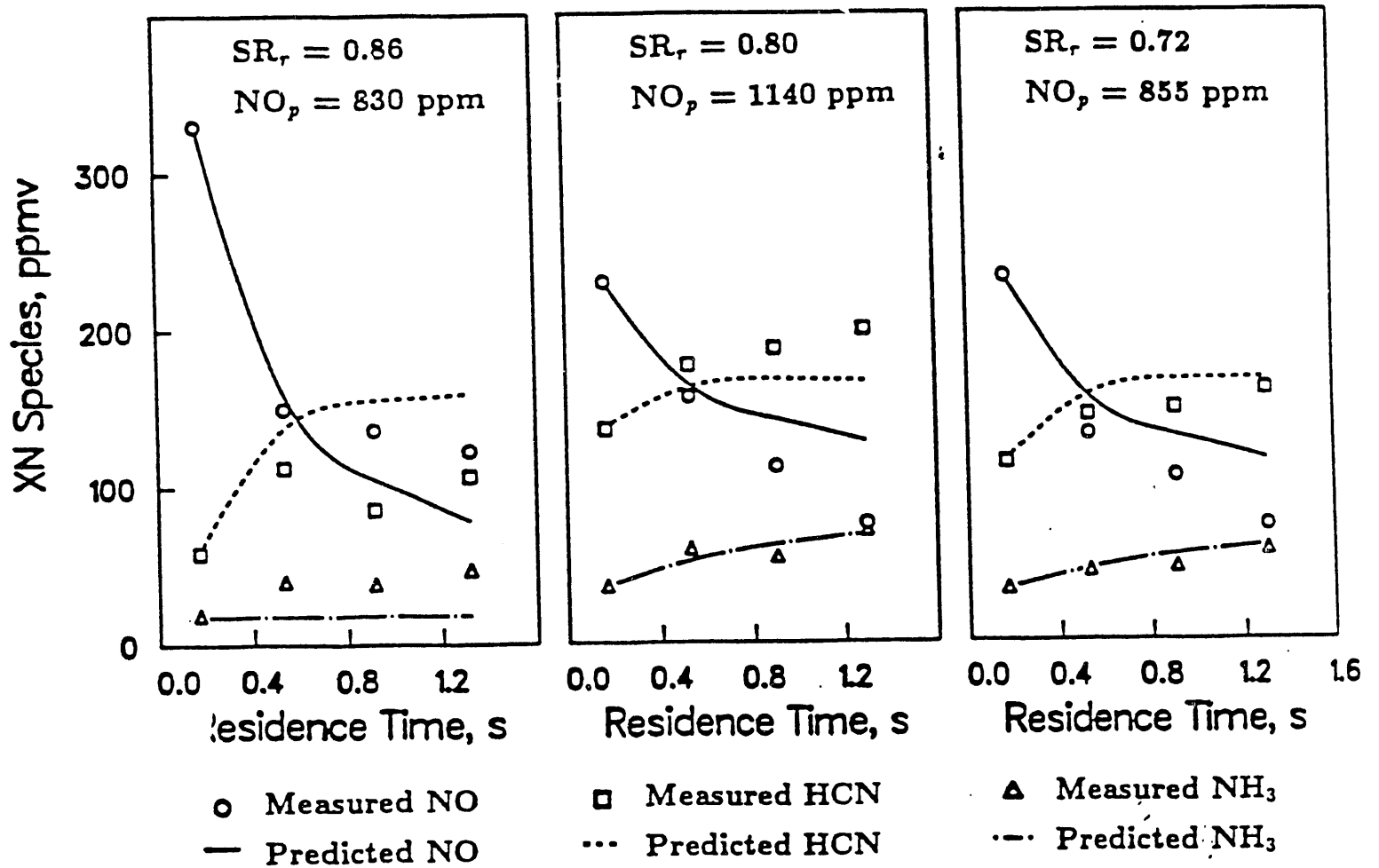
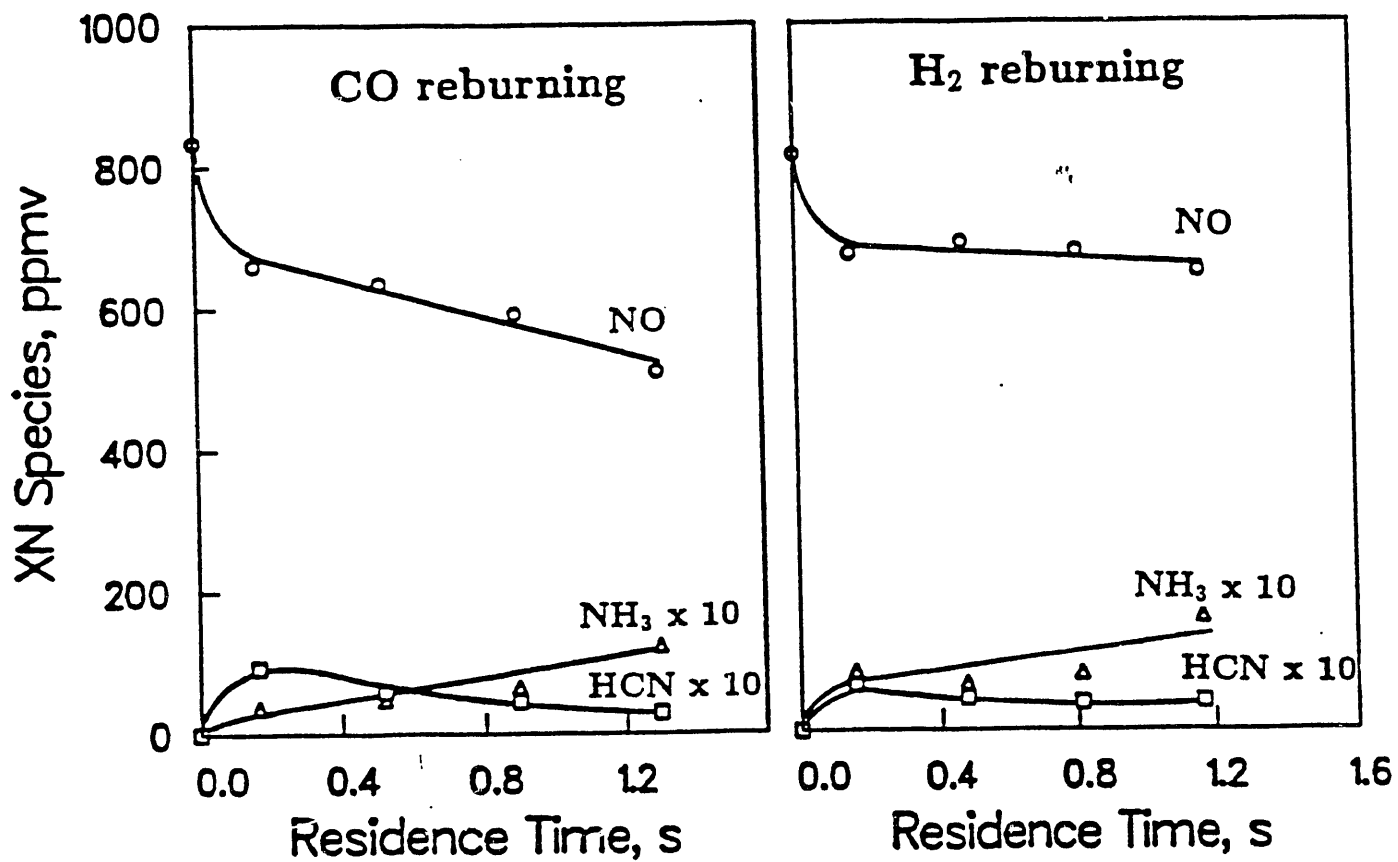FIG. 5.   Fixed Nitrogen Species Profiles in the Reburn Zone—Bituminous Coal/Natural Gas.

FIG. 6.   Fixed Nitrogen Species Profiles in the Reburn Zone—Bituminous Coal/Non–Hydrocarbon Gas for $SR_r = 0.90$ and $NO_p \approx 825$ ppm.
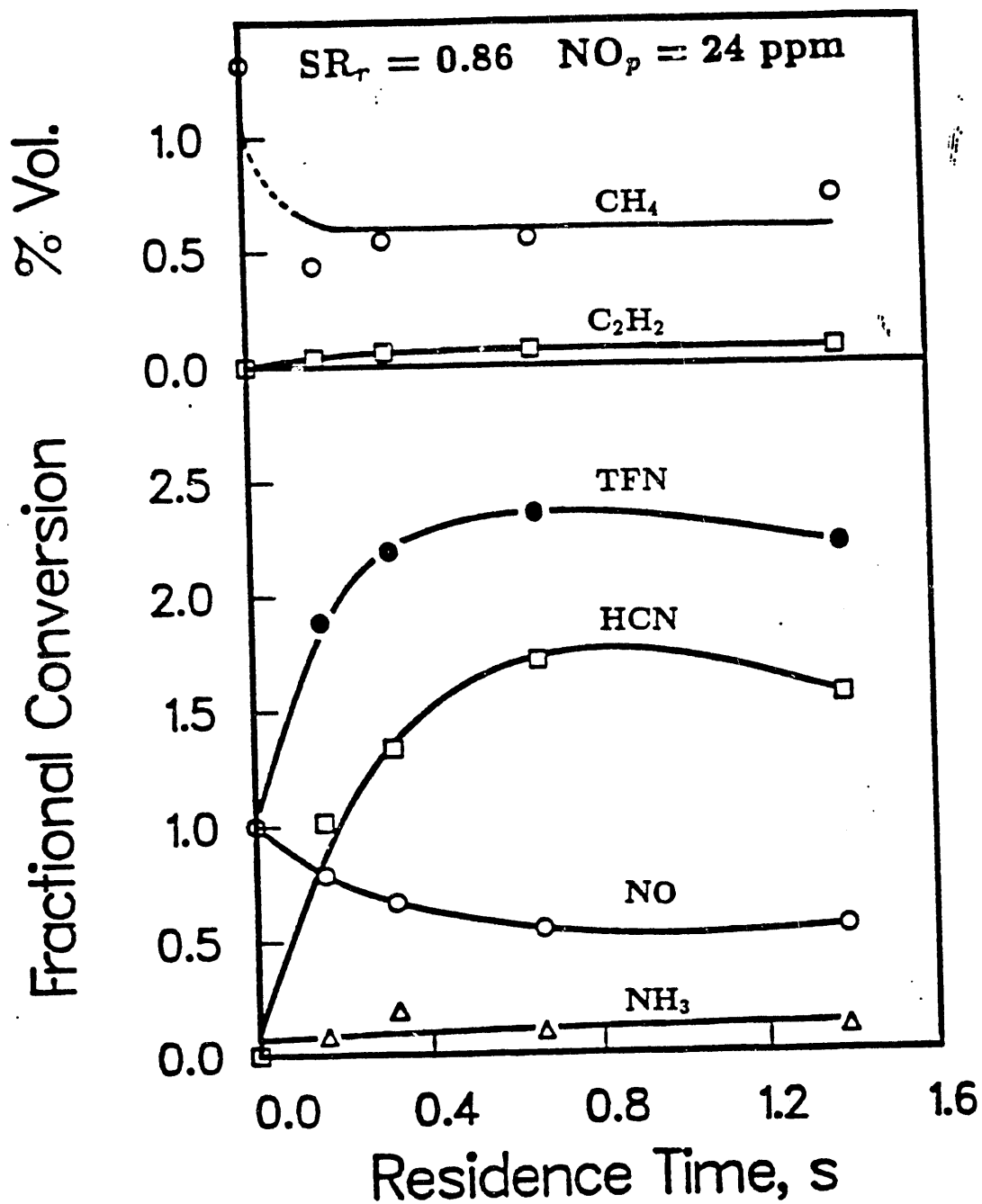
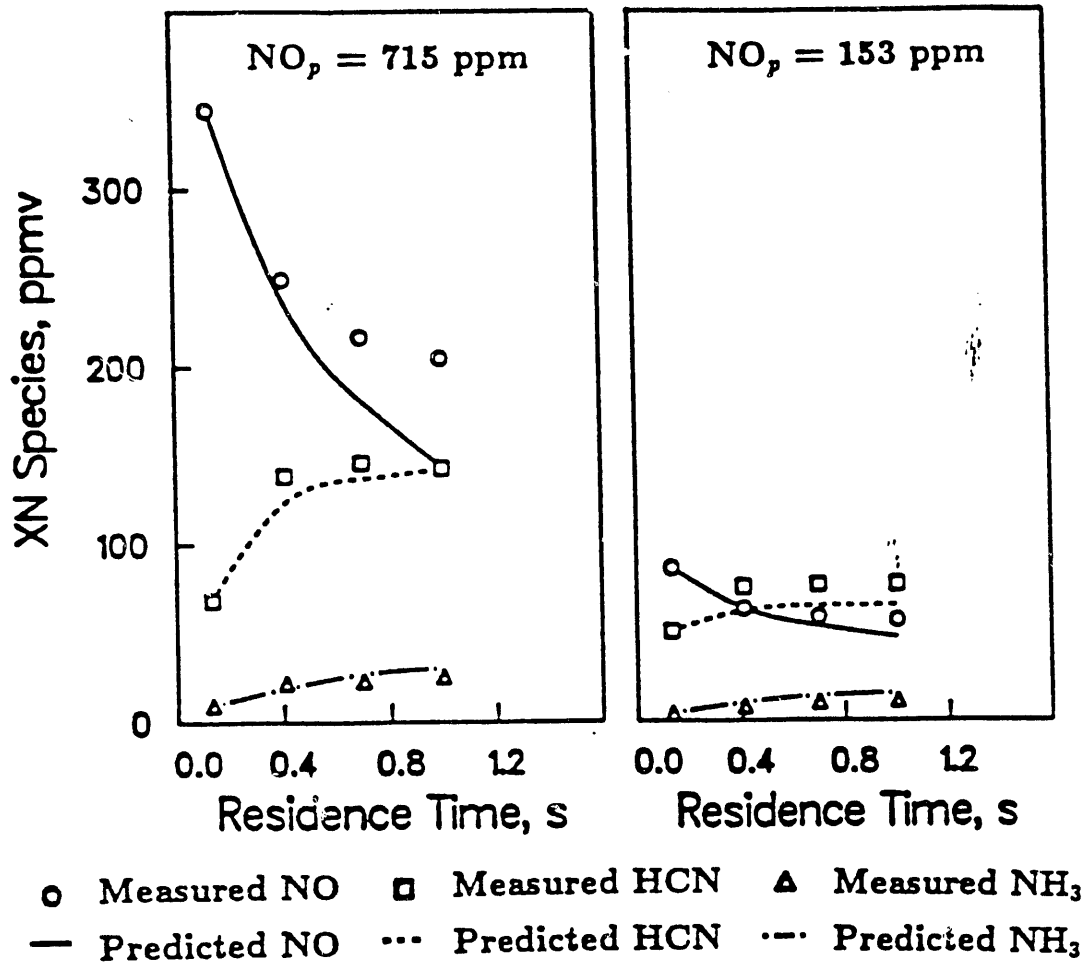FIG. 7.   Fixed Nitrogen Species Profiles in the Reburn Zone—Natural Gas/Natural Gas.

FIG. 8.   Fixed Nitrogen Species Profiles in the Reburn Zone—Natural Gas + NH_3/Natural Gas for $SR_r = 0.87$.

FIG. 9.   Fixed Nitrogen Species Profiles in the Reburn Zone—Bituminous Coal/Natural Gas.

Symbols – Experimental Data, Curves – Predictions.

A – Equilibrium OH model.

B – Empirical non-equilibrium OH model.

C – Kinetic OH model.

D – Kinetic OH model, expanded mechanism, see text.

FIG. 10.   Comparison between Model Predictions and Measurements.
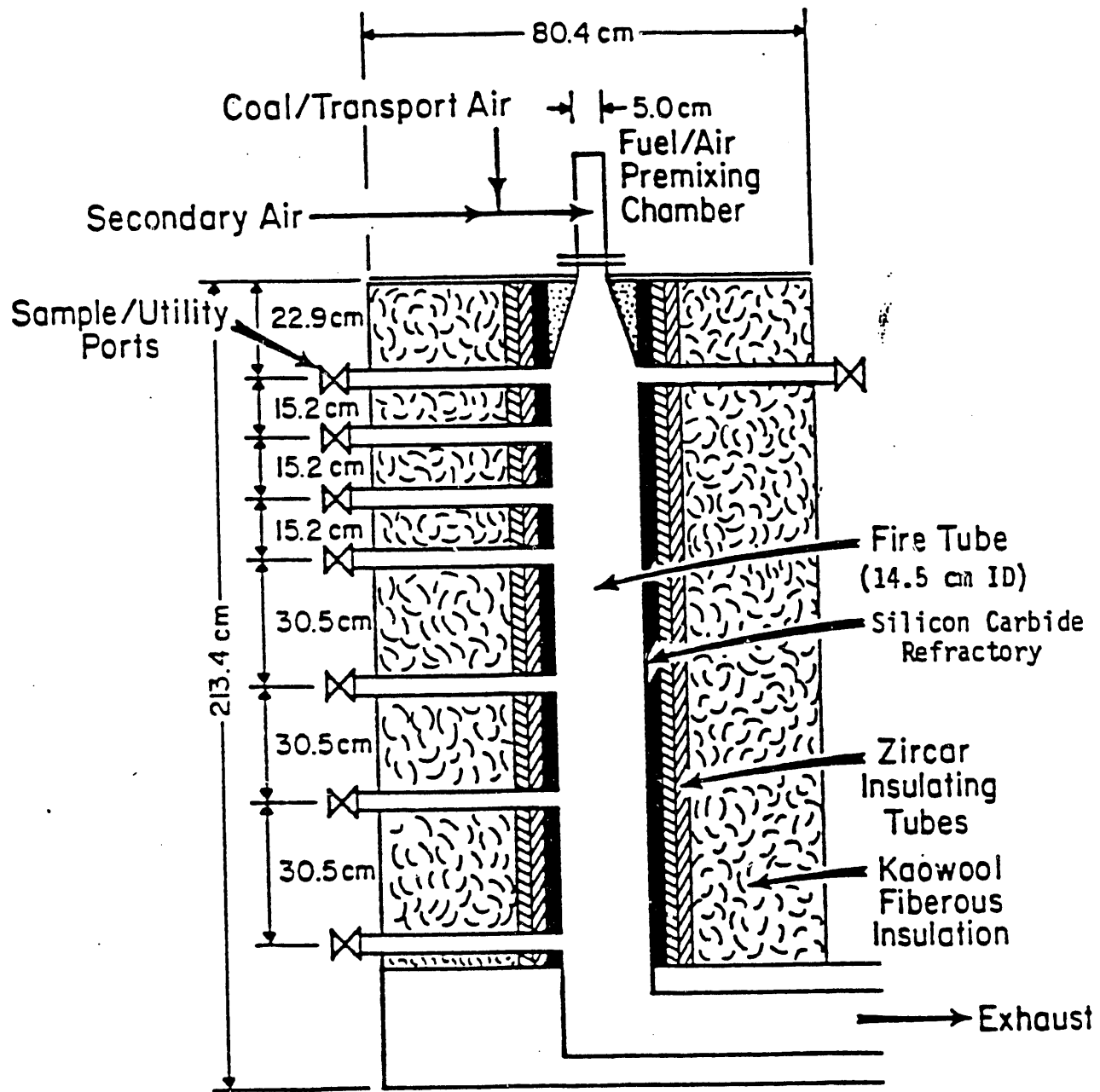
FIG. 1. Experimental Combustor

FIG. 2. Contour Plots for NO Reduction.

FIG. 3. *Variation of NO Reduction with Reburn Zone Stoichiometric Ratio and Temperature.*

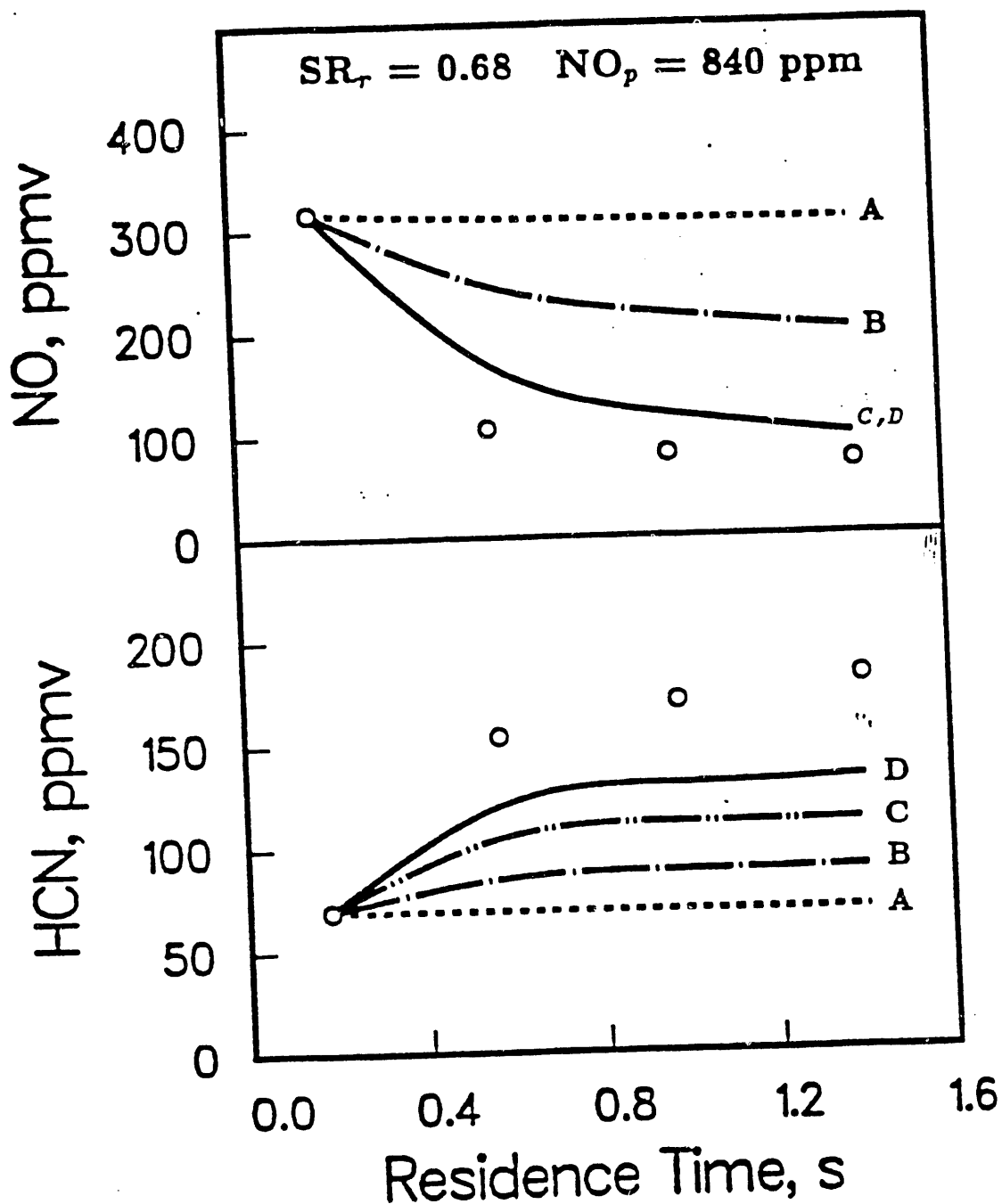FIG. 4. *Variation of NO Reduction with Reburn Zone Stoichiometric Ratio.*

FIG. 5. Fixed Nitrogen Species Profiles in the Reburn Zone—Bituminous Coal/Natural Gas.

FIG. 6. Fixed Nitrogen Species Profiles in the Reburn Zone–
Bituminous Coal/Non–Hydrocarbon Gas
for $SR_r = 0.90$ and $NO_p \approx 825$ ppm.

FIG. 7. Fixed Nitrogen Species Profiles in the Reburn Zone—

FIG. *8.* Fixed Nitrogen Species Profiles in the Reburn Zone–
Natural Gas + NH_3/Natural Gas for SR_r=0.87.

FIG. 9. Fixed Nitrogen Species Profiles in the Reburn Zone—
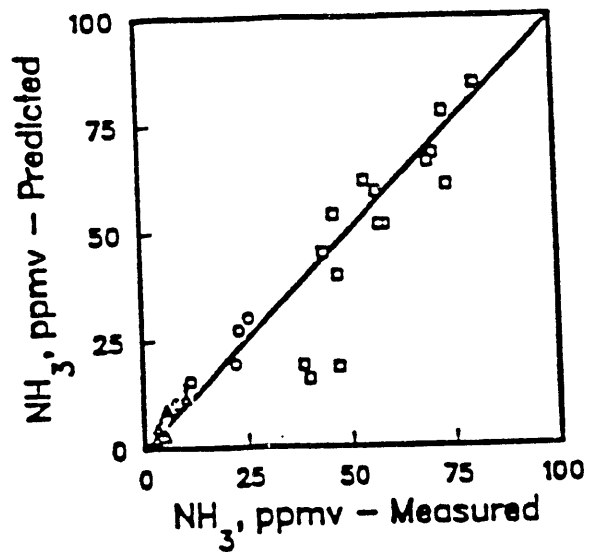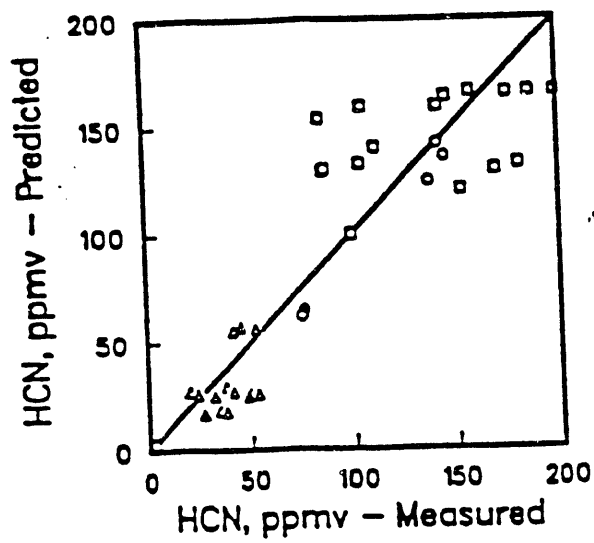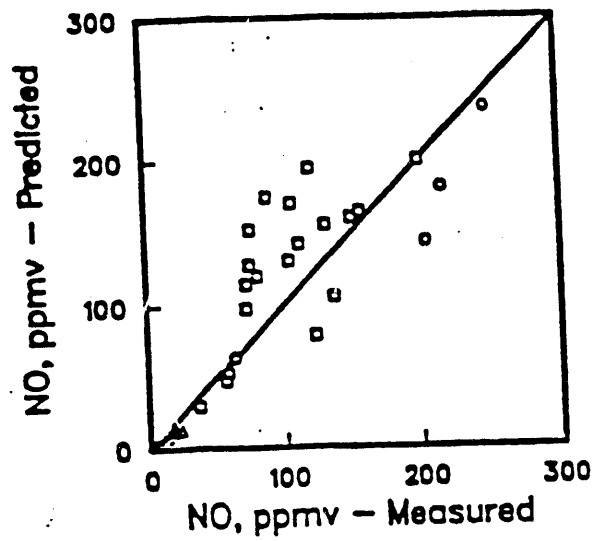Bituminous Coal/Natural Gas.

Symbols – Experimental Data, Curves – Predictions.

A – Equilibrium OH model.

B – Empirical non-equilibrium OH model.

C – Kinetic OH model.

D – Kinetic OH model, expanded mechanism, see text.

□ Utah Bituminous Coal/Natural Gas

○ Natural Gas + NH₃/Natural Gas

▲ Natural Gas/Natural Gas

FIG. 10. Comparison between Model Predictions and Measurements.

END

DATE FILMED

2/18/92